Magnitude and sign of long-range correlated time series: Decomposition and surrogate signal generation

Manuel Gómez-Extremera,[1] Pedro Carpena,[1] Plamen Ch. Ivanov,[2,3,4] and Pedro A. Bernaola-Galván[1]

[1]*Dpto. de Física Aplicada II, ETSI de Telecomunicación, University of Málaga, 29071 Málaga, Spain*

[2]*Keck Laboratory for Network Physiology, Department of Physics, Boston University, Boston, Massachusetts 02215, USA*

[3]*Harvard Medical School and Division of Sleep Medicine, Brigham and Women's Hospital, Boston, Massachusetts 02115, USA*

[4]*Institute of Solid State Physics, Bulgarian Academy of Sciences, 1784 Sofia, Bulgaria*

(Received 23 December 2015; published 4 April 2016)

We systematically study the scaling properties of the magnitude and sign of the fluctuations in correlated time series, which is a simple and useful approach to distinguish between systems with different dynamical properties but the same linear correlations. First, we decompose artificial long-range power-law linearly correlated time series into magnitude and sign series derived from the consecutive increments in the original series, and we study their correlation properties. We find analytical expressions for the correlation exponent of the sign series as a function of the exponent of the original series. Such expressions are necessary for modeling surrogate time series with desired scaling properties. Next, we study linear and nonlinear correlation properties of series composed as products of independent magnitude and sign series. These surrogate series can be considered as a zero-order approximation to the analysis of the coupling of magnitude and sign in real data, a problem still open in many fields. We find analytical results for the scaling behavior of the composed series as a function of the correlation exponents of the magnitude and sign series used in the composition, and we determine the ranges of magnitude and sign correlation exponents leading to either single scaling or to crossover behaviors. Finally, we obtain how the linear and nonlinear properties of the composed series depend on the correlation exponents of their magnitude and sign series. Based on this information we propose a method to generate surrogate series with controlled correlation exponent and multifractal spectrum.

DOI: 10.1103/PhysRevE.93.042201

I. INTRODUCTION

A wide variety of phenomena in different fields ranging from physiology to economy show complex dynamics generating output signals that appear to be erratic and noisy but that, in fact, possess long-range correlations with scale-invariant structure. In addition, it has been observed that the presence of such correlations is linked to relevant properties of the system under study; for example, the correlations in the series of heartbeats change from healthy to pathological conditions [1] or under different physiological states [2].

In many cases, given a time series $x_i, i = 1,2,\ldots,N$, its increments $\Delta x_i = x_{i+1} - x_i$ are more relevant than the series itself because the dynamical properties of the increments provide with interesting clues about the underlying dynamics of the system and could help to develop useful models.

For nonlinear systems it is important to go beyond the study of linear correlations because they do not account for all dynamical properties of such systems; e.g., increment time series with the same linear correlations could correspond to systems with completely different nonlinear and multifractal behaviors [3]. A simple approach to break this degeneration consists in studying separately the correlations of magnitude and sign of the increment time series. The correlations in the series of magnitudes (also known as volatility series) have been related to the presence of nonlinear correlations and multifractal structure [3–5], whereas the properties of the sign series are solely determined by the linear correlations [3,4] and have been studied in the context of first-passage time in scale-invariant correlated processes [6].

In addition, from the intuitive point of view, magnitude and sign time series contain different and complementary information about the original signal: the magnitude measures how big the changes are and the sign indicates their direction. An example of this is the dynamics of the heart [3], which is thought to be the result of two competing forces, the sympathetic and parasympathetic branches of the autonomous nervous system, that leads to complex variability with scale-invariant characteristics. Roughly speaking, the first one is responsible for slow (small in magnitude) increases (positive in sign) of the heart rate, while the second is usually associated with fast (large in magnitude) decreases (negative in sign). Other examples of the usefulness of the magnitude and sign analysis are also found in fluid dynamics [7], geological [8,9], geophysical [10,11], and economical time series [12].

Despite the importance of the magnitude and sign time series we have just mentioned, there are still open questions: for example, given a time series with known long-range correlations, a key question is whether there are correlations present also in the magnitude and sign time series? The approach to address this question is what we call here the *decomposition* problem. In principle, the systematic study of this problem is a complicated task, since the original time series can have very different nature, as mentioned above. Instead, we study the decomposition problem in artificial time series, which are commonly used to model the behavior of long-range correlated time series. In particular, we consider fractional Gaussian noises (fGns) and fractional Brownian motions (fBms) to model respectively stationary and nonstationary long-range correlated time series.

Furthermore, a second important problem (still open in many cases) is how the magnitude and sign of the increments are coupled to form the whole signal: for example, in

the human heart, when analyzing the increments of the interbeat interval time series, it is not clear yet what the relationship is between the magnitude (how big the change in the cardiac rhythm is) and the sign (the direction of the change). Obviously, a systematic study of the coupling between magnitude and sign series would be of great interest to improve the understanding of the relation between them and the behavior of the underlying mechanisms of control. Specifically, we investigate how the correlations of the whole signal are controlled by the correlations in the magnitude and sign time series, as well as by the coupling between them. However, the coupling mechanism of magnitude and sign will be different in time series of different nature, since the underlying dynamics will be different as well, and this variety of potential coupling mechanisms makes a systematic analysis difficult. Nevertheless, we can approach this problem from a different point of view: we can study systematically the correlation properties of time series with *uncoupled* magnitude and sign. Such time series can be artificially generated by multiplying magnitude and sign time series (each one with known correlations) obtained from different fGns or fBms. In this way, we guarantee that both magnitude and sign series are independent and thus uncoupled. Such analysis is what we call here the *composition problem*. The composition problem can be useful to understand the behavior of complex systems characterized by the coupling of two different mechanisms, each controlling the dynamics of magnitude and sign respectively. In addition, the results of the composition problem are a reference of uncoupling and then can be used to detect the existence of coupling mechanisms when analyzing real complex time series.

This article is organized as follows: In Sec. II we describe the methods and algorithms used in this article. Specifically, in Sec. II A we describe Detrended Fluctuation Analysis (DFA), the method used here to quantify the linear correlations, in Sec. II B we explain Multifractal Detrended Fluctuation Analysis (MFDFA), the algorithm we use to obtain multifractal spectra of time series, and Sec. II C introduces the Fourier Filtering Method, which allows us to generate signals with given correlation exponent.

In Sec. III we systematically study the decomposition problem, i.e., the correlation properties of the magnitude and sign time series obtained from long-range power-law linearly correlated time series. In Sec. IV we investigate the composition problem; i.e., we systematically study the correlations properties of composed time series with uncoupled magnitude and sign series. The multifractal properties of such composed series are analyzed in Sec. V, and, finally, Sec. VI presents the conclusions of this work.

II. METHODS

A. Detrended Fluctuation Analysis (DFA)

Here we quantify the linear correlations of time series by using Detrended Fluctuation Analysis (DFA) [13], a modified version of Fluctuation Analysis (FA), which is able to eliminate the effects of the nonstationarity. This method provides a single quantitative parameter, the scaling exponent α, to represent the correlation properties of a long-range correlated series.

DFA consists of the following steps [13]:

(i) Starting with a correlated series $\{x_i\}$ of size N we first integrate the series and obtain

$$y(j) \equiv \sum_{i=1}^{j} [x_i - \mu], \tag{1}$$

where μ is the mean value of the entire series.

(ii) The integrated series $y(j)$ is divided into boxes of equal length ℓ.

(iii) In each box of length ℓ, we calculate a linear fit of $y(j)$ which represents the *linear trend* in that box. The y coordinate of the fit line in each box is denoted by $y_\ell(j)$.

(iv) The integrated series $y(j)$ is detrended by subtracting the local trend $y_\ell(j)$ in each box of length ℓ.

(v) For a given box size ℓ, the root mean square (r.m.s.) fluctuation for this integrated and detrended series is calculated:

$$F(\ell) = \sqrt{\frac{1}{N} \sum_{j=1}^{N} [y(j) - y_\ell(j)]^2}. \tag{2}$$

(vi) The above computation is repeated for a broad range of scales (box sizes ℓ) to provide a relationship between $F(\ell)$ and the box size ℓ.

For a power-law correlated time series, there exists a power-law relation between the average root-mean-square fluctuation function $F(\ell)$ and the box size ℓ: $F(\ell) \sim \ell^\alpha$. Thus, the fluctuations can be characterized by a scaling exponent α, a self-similarity parameter which quantifies the long-range power-law correlation properties of the signal.

If the power-law correlated time series is stationary ($\alpha < 1$), the autocorrelation function decays as a power law, $C(\ell) \sim \mathrm{sgn}(1-\gamma)/\ell^\gamma$, and the exponent α is related to the exponent γ by [14–16]

$$\alpha = \frac{2-\gamma}{2}. \tag{3}$$

Note that for the special case $\gamma = 1$ ($\alpha = 0.5$) the autocorrelation function vanishes.

In addition, it can be shown, via the Wiener-Khinchin theorem, that the power spectrum of the series is also a power law, whose exponent β is indeed related to α [16]:

$$\alpha = \frac{\beta+1}{2}. \tag{4}$$

Here it is worth mentioning that, although Wiener-Khinchin theorem is only for $\alpha < 1$, this relationship between α and β is also valid for $\alpha > 1$.

Values of $\alpha < 0.5$ indicate the presence of anticorrelations in the time series, $\alpha = 0.5$ absence of correlations (white noise) and $\alpha > 0.5$ indicates the presence of positive correlations in the time series. In particular, for $\alpha = 1.5$ the series correspond to the well-known Brownian motion.

The performance of DFA has been systematically studied for time series with different trends [17,18], missing data [19], different artifacts [20], linear and nonlinear preprocessing filters [21], and coarse graining of the time series values [22].

B. Multifractal Detrended Fluctuation Analysis (MFDFA)

DFA studies the scaling of the second-order moment as a function of the window size ℓ, and thus, it takes into account only the linear correlations present in the series. MFDFA can be understood as a generalization of DFA in the sense that it analyzes the scaling of all possible moments of order q (including negative ones) [23]. To do so, Eq. (2) is generalized as follows:

$$F_q(\ell) = \left[\frac{1}{N} \sum_{j=1}^{N} |y(j) - y_\ell(j)|^q \right]^{\frac{1}{q}}. \tag{5}$$

For long-range power-law correlated time series, the fluctuations $F_q(\ell)$ scale as a power law of the form

$$F_q(\ell) \sim \ell^{h(q)}, \tag{6}$$

where $h(q)$ is the scaling exponent of the fluctuations of order q as a function of the window size ℓ. Obviously, the DFA exponent α is a particular case for $q = 2$, i.e., $\alpha = h(2)$. For series with only linear correlations $h(q) = \alpha \ \ \forall q$, i.e., there is a single scaling exponent and the series is *monofractal*. On the other hand, when nonlinear correlations are present in the series, each moment scales with a different exponent $h(q)$ and the series will be *multifractal*.

The scaling exponents $h(q)$ can be related to the classical multifractal box-counting scaling exponents $\tau(q)$ by means of the expression

$$\tau(q) = qh(q) - 1. \tag{7}$$

Finally, calculating the Lengendre transform we can obtain the multifractal spectrum (see Ref. [23]):

$$\zeta = \tau'(q), \tag{8}$$

$$f(\zeta) = q\zeta - \tau(q), \tag{9}$$

where $f(\zeta)$ denotes the fractal dimension of the subset of the series characterized by ζ. For the particular case of monofractal time series, as all the moments scale with the same exponent, $h(q) = \alpha, h'(q) = 0$, and the multifractal spectrum will be a delta function:

$$f(\zeta) = \delta(\zeta - \alpha). \tag{10}$$

In contrast, for a multifractal series, $f(\zeta)$ will have a nonzero width, $\Delta\zeta$, which can be used as a measure of the strength of the nonlinearities present in the series.

C. Fourier Filtering Method

To generate artificial series with long-range power-law correlations we use the Fourier Filtering Method (FFM) [24,25]. This method makes use of Eq. (4) to obtain a series with DFA exponent α.

It works as follows:

(i) Generate a white noise $\eta(i)$, i.e., a series of uncorrelated Gaussian-distributed numbers all with the same mean and variance, and compute its Fourier transform, $\hat{\eta}(f)$.

(ii) The series with the desired correlation exponent α is obtained as

$$x(i;\alpha) \equiv \mathcal{F}^{-1}\left[\frac{\hat{\eta}(f)}{f^{\alpha-1/2}} \right], \tag{11}$$

where $\mathcal{F}^{-1}[\cdot]$ denotes the inverse Fourier transform. To check this, simply take into account that the Fourier transform of $x(i;\alpha)$ is a power law of exponent $\alpha - 1/2$ and thus its power spectrum follows a power law with exponent $2\alpha - 1$, which, according to Eq. (4), gives a DFA exponent α. Time series generated by FFM are normalized to zero mean and unit variance.

III. DECOMPOSITION OF A TIME SERIES: CORRELATIONS IN THE MAGNITUDE AND SIGN

Our aim is to quantify the correlations in the magnitude and sign time series obtained from the decomposition of a long-range correlated time series with a given input correlations. To systematically analyze the correlation properties of the magnitude and sign series, we generate artificial series of length $2^{20} \simeq 10^6$ using FFM with different input values of the correlation exponent (α_{in}) equally spaced in the (0,2) interval. Figure 1 shows an example of a correlated series obtained for $\alpha_{\text{in}} = 1$, as well as its magnitude and sign series.

For each individual series we obtain its corresponding magnitude and sign series, compute their correlation exponents (α_{mag} and α_{sign} respectively), and average them over an ensemble of 200 experiments for each input α_{in} value. We also compute the correlation exponent of the generated time series (α_{out}), which could be slightly different from α_{in} due to statistical fluctuations and finite size effects (Fig. 2).

In Fig. 3 we show the results. We observe three different regions:

(i) $\alpha_{\text{in}} \leqslant 0.5$. Despite the anticorrelations of the time series, both magnitude and sign are essentially uncorrelated. In all cases the magnitude series show a perfect fit to a power law with exponent $\alpha_{\text{mag}} = 0.5$ for all considered scales. These series are virtually indistinguishable from random i.i.d. series. But, on the other hand, the sign series (especially for $\alpha_{\text{in}} > 0.2$)

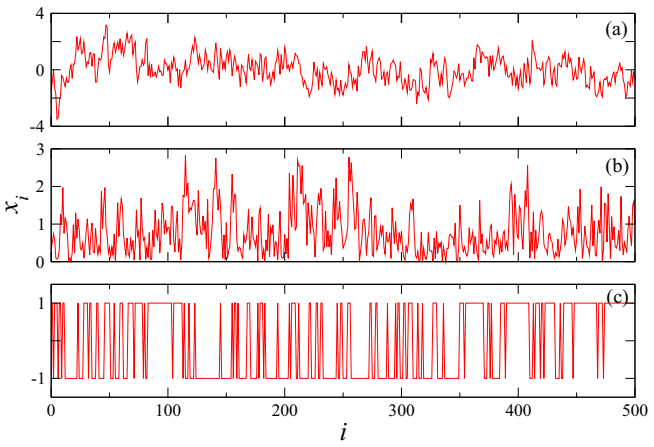

FIG. 1. (a) Example of correlated series obtained with the Fourier filtering method and $\alpha_{\text{in}} = 1$. (b) Series of its magnitudes and (c) series of its signs.

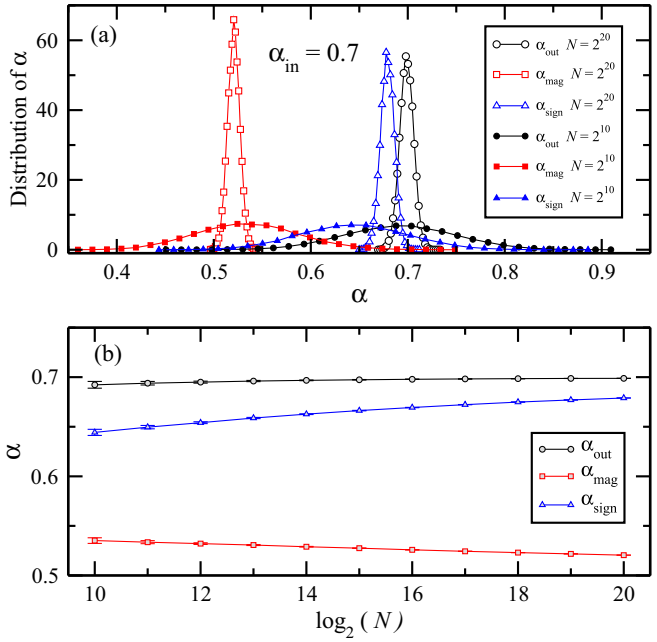

FIG. 2. Finite size effects. (a) Distributions of α_{out}, α_{mag}, and α_{sign} for two ensembles of 65 000 series generated by using the FFM with $\alpha_{in} = 0.7$. Open symbols: length of the series $N = 2^{20} \simeq 10^6$, full symbols: length of the series $N = 2^{10} \simeq 10^3$. Due to statistical fluctuations, the values of the correlation exponent α_{out} are not exactly equal to α_{in}; instead they are normally distributed with a variance that decreases as N increases. A similar behavior is observed for α_{mag} and α_{sign}. (b) Mean values and standard deviations (error bars) of the distributions of of α_{out},α_{mag}, and α_{sign} for experiments similar to those in (a) for series size ranging from $N = 2^{10}$ to $N = 2^{20}$. In all three cases the mean values seem to approach an asymptotic value as N grows. In particular, both α_{out} and α_{sign} tend to the same value, α_{in}, the convergence being slower for α_{sign}. The fact that α_{out} and α_{sign} have the same asymptotic limit is observed only within the region $0.5 \leqslant \alpha_{in} < 1$, whereas in the region $\alpha_{in} > 1$,α_{mag} tends asymptotically to the same limit as α_{out} (see Sec. III).

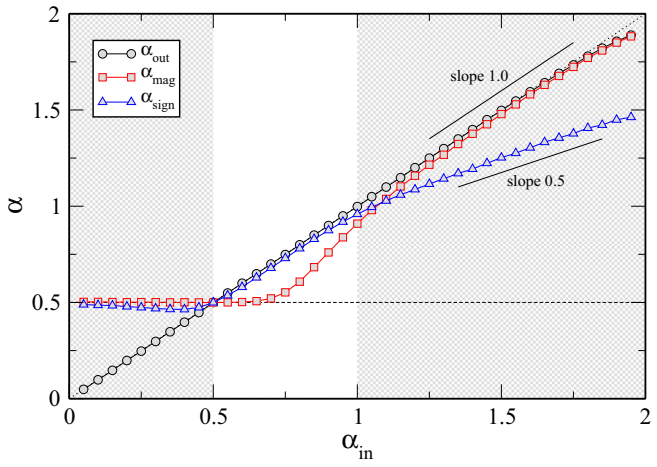

FIG. 3. Averaged correlation exponents for the composed signal (α_{out}), magnitude (α_{mag}), and sign (α_{sign}) as a function of α_{in}. For each value of α_{in} we generate 200 series of length $N = 2^{20}$ to obtain the averages.

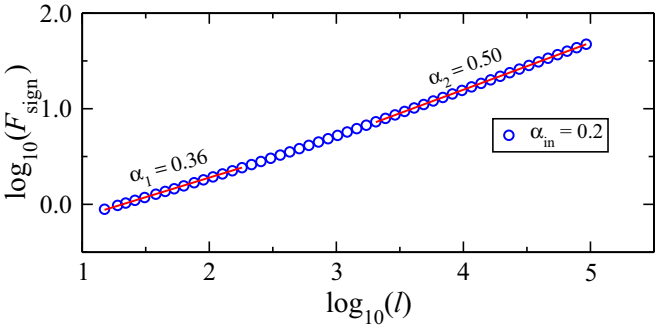

FIG. 4. $F_{sign}(\ell)$ vs ℓ for the sign series in the region $\alpha_{in} \leqslant 0.5$. We average $F_{sign}(\ell)$ over an ensemble of 200 sign series obtained from anticorrelated series of size $N = 2^{20}$ and $\alpha_{in} = 0.2$. The global scaling exponent, $\alpha_{sign} = 0.46$, indicates the presence of anticorrelations, but the direct inspection of $F_{sign}(\ell)$ reveals the existence of a crossover around $\ell_c = 190$. Below ℓ_c the sign series exhibits anticorrelations ($\alpha_1 = 0.36$), but such behavior disappears for $\ell > \ell_c$ ($\alpha_2 = 0.50$).

show values of $\alpha_{sign} \lesssim 0.5$ thus implying the presence of anticorrelations.

We find that only at short scales sign series show clear anticorrelated behavior, while at intermediate and large scales, the behavior is uncorrelated. This effect is shown in Fig. 4, where we plot the typical behavior of $F_{sign}(\ell)$ for the sign series in the region $\alpha_{in} \leqslant 0.5$. At small ℓ, $F_{sign}(\ell)$ scales with exponent $\alpha_1 = 0.36$ and, after a transition regime, the rest of the curve shows an scaling exponent $\alpha_2 = 0.50$ corresponding to uncorrelated behavior.

For this reason, the global exponent α_{sign}, obtained as a fit for the whole ℓ range (Fig. 3), is affected by these first values of the $F_{sign}(\ell)$ curve, thus leading to $\alpha_{sign} \lesssim 0.5$.

In summary, for large enough scales, both magnitude and sign series are uncorrelated. Having this in mind, the anticorrelations in the series (present at all scales) must be a result of the coupling between magnitude and sign because none of them are significantly anticorrelated themselves. To check this, we perform the following experiment: Generate a signal with $\alpha_{in} = 0.3$, decompose it into its magnitude and sign series, shuffle the sign (thus destroying all possible coupling between magnitude and sign), and finally multiply the randomized sign series by the original magnitude series to obtain a surrogate signal with uncoupled magnitude and sign. We also do the same experiment but randomizing the magnitude series. The results shown in Fig. 5 confirm our initial guess: the two surrogate series lose their anticorrelations since $F(\ell)$ scales as $\ell^{0.5}$. Note that in the second experiment, where we randomized the magnitude, the surrogate series still preserves certain anticorrelations at small scales coming from those present in the original sign series. Nevertheless, for ℓ large enough, the random behavior is recovered and the fluctuations scale with $\alpha = 0.5$.

An important conclusion drawn from here is the fact that it is not possible to obtain long-range anticorrelated binary sequences from the sign of an anticorrelated time series. This limitation has also been found in other methods described in the bibliography for the generation of long-range correlated binary sequences [26–28].

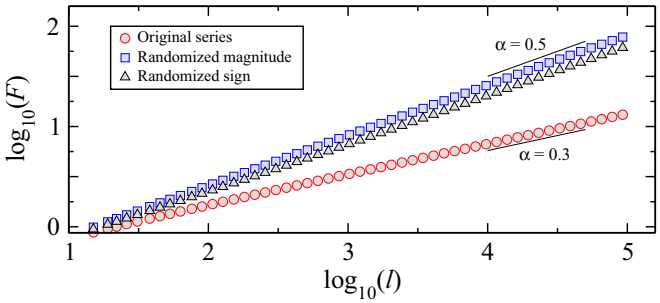

FIG. 5. $F(\ell)$ vs ℓ for anticorrelated series ($\alpha_{\text{in}} = 0.3$) and for surrogate series obtained by means of sign or magnitude randomization: Generate a sign with $\alpha_{\text{in}} = 0.3$, decompose it into its magnitude and sign series, randomize the sign or magnitude series, and obtain two surrogate series, one multiplying the randomized sign by the original magnitude (△) and the other multiplying the randomized magnitude by the original sign (□). Both curves have been obtained for signals with $N = 2^{20}$ and averaging over 200 experiments.

(ii) $0.5 < \alpha_{\text{in}} < 1$. In this region sign series show correlations in the whole interval, while magnitude series are correlated only beyond $\alpha_{\text{in}} = 0.75$. Nevertheless, the correlations in the original signal are controlled by those in the sign no matter if the magnitude series are correlated or not. These results are in agreement with Ref. [29], where an analytical relation between $C(\ell)$ and $C_{\text{sign}}(\ell)$ was found:

$$C(\ell) = \sin\left[\frac{\pi}{2} C_{\text{sign}}(\ell)\right] \tag{12}$$

valid for $\gamma < 1$ and $C(\ell) > 0$, i.e., $0.5 < \alpha < 1$. Taking into account that the correlations will be much smaller than one for large enough ℓ, the sine in Eq. (12) can be approximated by its argument, and, assuming power-law dependence for the autocorrelation function, we get

$$\frac{1}{\ell^{\gamma_{\text{out}}}} \simeq \frac{\pi}{2} \frac{1}{\ell^{\gamma_{\text{sign}}}}, \tag{13}$$

and using (3) we obtain

$$\alpha_{\text{sign}} \simeq \alpha_{\text{out}} - \frac{\log(\pi/2)}{2\log \ell}. \tag{14}$$

Note that, according to Eq. (14), in Fig. 3, α_{sign} is always slightly smaller than α_{out}. In fact, $\alpha_{\text{sign}} \to \alpha_{\text{out}}$ only asymptotically [see Fig. 2(b)]. This behavior has been already observed by Carretero-Campos *et al.* [6] studying the sign series in the context of the distribution of first-passage times in correlated time series.

Within this region, sign series provide an easy method to obtain correlated binary sequences with a correlation exponent α_{sign}, which is virtually the same as the exponent of the original series α_{in}. For example, this method is useful to study DNA sequences that have been frequently modeled as correlated binary sequences with correlation exponents $0.5 < \alpha < 1$ [30].

Here, contrary to what we observed in the previous region, the coupling between magnitude and sign does not seem to play a relevant role. Indeed, as we will show in Sec. IV, even under the assumption of independence between magnitude and sign, the correlations of the signal are controlled by those in the sign, as long as $\alpha_{\text{mag}}, \alpha_{\text{sign}} \in (0.5, 1)$.

(iii) $1 < \alpha_{\text{in}} < 2$. Both α_{mag} and α_{sign} continue increasing with α_{in}. Now, α_{mag} is the one which tends asymptotically to α_{out}; i.e., in this region correlations of the composed signal are controlled by the magnitude. On the other hand, α_{sign} grows as a function of α_{in} with slope $1/2$; thus, in this region:

$$\alpha_{\text{sign}} = \tfrac{1}{2}(1 + \alpha_{\text{in}}). \tag{15}$$

This behavior can be explained analytically by using the properties of the distribution of first-passage times for linearly correlated series found in Ref. [6]. It is also easy to show that α_{sign} cannot be larger than $3/2$ (see Appendix A for a proof of both properties).

In summary, we have for the correlation exponent α_{sign} as a function of α_{in} the next asymptotic behavior:

$$\alpha_{\text{sign}} = \begin{cases} \frac{1}{2} & \alpha_{\text{in}} < \frac{1}{2} \\ \alpha_{\text{in}} & \frac{1}{2} \leqslant \alpha_{\text{in}} < 1 \\ \frac{1}{2}(1 + \alpha_{\text{in}}) & 1 \leqslant \alpha_{\text{in}} < 2 \\ \frac{3}{2} & 2 \leqslant \alpha_{\text{in}} \end{cases}. \tag{16}$$

For the correlation exponent α_{mag} the asymptotic behavior consists of an uncorrelated zone for $\alpha_{\text{in}} < \frac{3}{4}$, a transition for $\frac{3}{4} < \alpha_{\text{in}} < \frac{5}{4}$, and a region where $\alpha_{\text{mag}} \simeq \alpha_{\text{in}}$ for $\alpha_{\text{in}} > \frac{5}{4}$. The correlations observed for the series of magnitudes $|\Delta x_i|$ are in good agreement with those obtained for the series $(\Delta x_i)^2$ in Ref. [5].

IV. COMPOSITION OF MAGNITUDE AND SIGN SERIES

As we stated in the introduction, we are also interested in the properties of the composition of independent series of correlated signs and magnitudes. Our interest is double: On the one hand, we study the behavior of time series whose magnitude and sign are controlled by independent mechanisms. One of them controls the magnitudes of the increments while their signs are controlled by the other. This can be considered as the simplest approach to model real signals. On the other hand, by understanding the behavior of time series with independent magnitude and sign, we are able to identify when magnitude and sign are not independent, and consequently, we can establish a coupling detection method. Thus, by investigating the correlation properties of such composed time series, we can elucidate whether the magnitude and sign of a real time series are uncoupled or not.

The procedure to generate a composed time series with independent magnitude and sign works as follows. In order to obtain independent series of magnitude and sign, using FFM we generate two independent correlated series with input correlation exponents α_{in1} and $\alpha_{\text{in2}}, x(i;\alpha_{\text{in1}})$ and $x(i;\alpha_{\text{in1}})$ respectively. Then the magnitude series is obtained as

$$x_{\text{mag}}(i) = |x(i;\alpha_{\text{in1}})|, \tag{17}$$

whose correlation exponent, α_{mag} depends on α_{in1} (Fig. 3). Correspondingly, we obtain the sign series as

$$x_{\text{sign}}(i) = \text{sgn}[x(i;\alpha_{\text{in2}})], \tag{18}$$

whose correlation exponent $\alpha_{\rm sign}$ depends on $\alpha_{\rm in2}$ (Fig. 3). Finally, the composed series is given by

$$x_{\rm comp}(i) = x_{\rm mag}(i) \cdot x_{\rm sign}(i). \tag{19}$$

Here we systematically study the correlations of the composed series with $\alpha_{\rm in1}$,$\alpha_{\rm in2}$ in the range [0.5,2] leading to $\alpha_{\rm mag} \in [0.5,1.5]$ and $\alpha_{\rm sign} \in [0.5,2]$ (Fig. 3). Note that we do not explore the region $\alpha_{\rm in1},\alpha_{\rm in2} < 0.5$ because, as we have shown above, for these values both magnitude and sign are essentially uncorrelated. Depending on $\alpha_{\rm mag}$ and $\alpha_{\rm sign}$ we have observed three different behaviors.

A. Case $\alpha_{\rm sign} < 1$

Here, independently of the exponent $\alpha_{\rm mag}$, the correlations in the composed series are controlled by those in the sign. Given a time series obtained as the product of two independent magnitude and sign series we show in Appendix B that its autocorrelation function can be written as

$$C(\ell) = C_{\rm sign}(\ell)\frac{(\pi-2)C_{\rm mag}(\ell)+2}{\pi}, \tag{20}$$

where $C(\ell)$,$C_{\rm mag}(\ell)$, and $C_{\rm sign}(\ell)$ are the autocorrelation functions of the composed signal at distance ℓ, its magnitude, and its sign, respectively.

Depending on $\alpha_{\rm mag}$ we distinguish two regimes:

(i) $\alpha_{\rm mag} < 1$. If the series are power-law correlated we have

$$C_{\rm mag}(\ell) \sim \ell^{-\gamma_{\rm mag}} \quad \text{and} \quad C_{\rm sign}(\ell) \sim \ell^{-\gamma_{\rm sign}}, \tag{21}$$

where $\gamma_{\rm mag} = 2\alpha_{\rm mag} - 2$ and $\gamma_{\rm sign} = 2\alpha_{\rm sign} - 2$ according to (3). Using Eq. (21) in Eq. (20) we have for the autocorrelation of the composed signal:

$$C(\ell) \sim \frac{\pi-2}{\pi}\ell^{-(\gamma_{\rm mag}+\gamma_{\rm sign})} + \frac{2}{\pi}\ell^{-\gamma_{\rm sign}}. \tag{22}$$

As we are considering $\alpha_{\rm mag},\alpha_{\rm sign} \in [0.5,1)$, it follows that $\gamma_{\rm sign} < \gamma_{\rm mag} + \gamma_{\rm sign}$, and thus, the second term will be the leading one for large enough ℓ:

$$C(\ell) \sim C_{\rm sign}(\ell). \tag{23}$$

(ii) $\alpha_{\rm mag} \geqslant 1$. Now $C_{\rm mag}(\ell) = $ constant and it follows straightforwardly from (20) that

$$C(\ell) \propto C_{\rm sign}(\ell). \tag{24}$$

Here it is important to note that while (23) is an approximation valid only for large enough ℓ, (24) holds in the whole range.

In Fig. 6 we show an example of such situations. For a fixed value $\alpha_{\rm mag}$ we obtain composed series with different values of $\alpha_{\rm sign}$, and, in all cases, the resulting correlation exponent is almost the same as $\alpha_{\rm sign}$ in agreement with Eqs. (23) and (24). According to this, we are able to generate artificial signals with the desired correlation exponent (controlled by $\alpha_{\rm sign}$) independently of the correlations in the magnitude series. As the correlations in the magnitude are known to be related to the nonlinear properties of the signal [5] this implies that we can control the linear and nonlinear properties of the composed signal (see Sec. V).

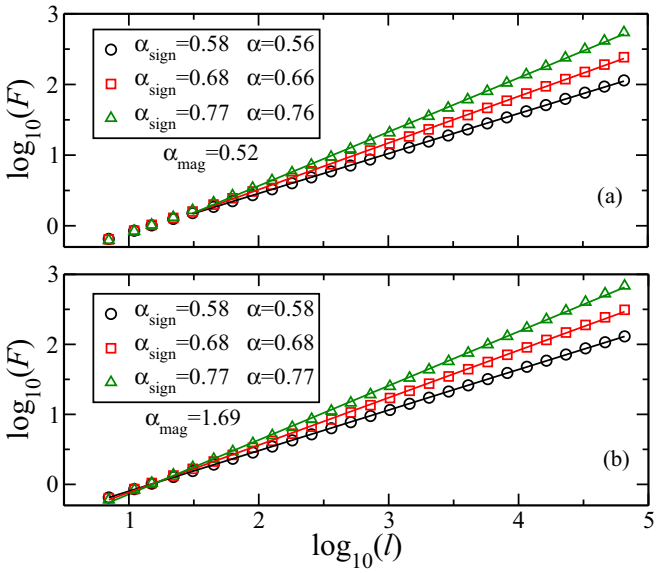

FIG. 6. Example of composed series generated by multiplying sign and magnitude from independent original series for $\alpha_{\rm sign} < 1$. (a) $\alpha_{\rm mag} < 1$. For ℓ large enough ($\ell > 30$) $F(\ell)$ scales with $\alpha \simeq \alpha_{\rm sign}$ according to Eq. (23). (b) $\alpha_{\rm mag} > 1$. $F(\ell)$ scales with $\alpha = \alpha_{\rm sign}$ in the whole range. Note that, contrary to Eq. (23), Eq. (24) is not an approximation for large ℓ. The size of the time series is 2^{20}, and the results are averaged over 200 experiments.

B. Case $\alpha_{\rm mag} < 1, \alpha_{\rm sign} > 1$

Here we observe different behaviors at short and large scales (Fig. 7). While for small ℓ the correlation exponent $\alpha_1 \simeq \alpha_{\rm mag}$, at large scales, the sign series takes over, and we get $\alpha_2 \simeq \alpha_{\rm sign}$. The reason for this scaling crossover can be explained as follows: Taking into account that $\alpha_{\rm sign} > 1$, a change of sign within a window of small size is unlikely to happen [6]; thus

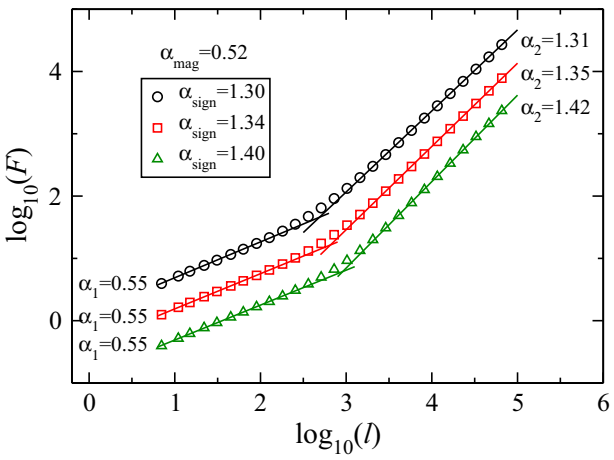

FIG. 7. Examples of composed series generated by multiplying sign and magnitude from independent original series for the case $\alpha_{\rm mag} < 1$ and $\alpha_{\rm sign} > 1$. We obtain a crossover ℓ dividing the range into two regions with different scaling: $\alpha_1 \simeq \alpha_{\rm mag}$ for $\ell < \ell_{\rm c}$ and $\alpha_2 \simeq \alpha_{\rm sign}$ for $\ell > \ell_{\rm c}$. The size of the time series is 2^{20}, and the results are averaged over 200 experiments. Different $F(\ell)$ have been shifted vertically for the sake of clarity.

the fluctuations at such scales depend only on the fluctuations of the magnitude. On the other hand, for large enough scales, the changes of the sign inside a single window will create fluctuations much higher than those of the magnitude, and thus, the correlation exponent will be close to $\alpha_{\rm sign}$.

The position of the crossover $\ell_{\rm c}$ between both regimes depends on the size N of the series and can be determined analytically taking into account that the transition between these two regions should happen at a window size $\ell_{\rm c}$ for which the fluctuations due to the oscillations of both sign and magnitude give the same contribution.

A long-range correlated series with $\alpha < 1$ is stationary, so we can write for the fluctuations in the magnitude at scale ℓ

$$F_{\rm mag}(\ell) = A_{\rm mag}\ell^{\alpha_{\rm mag}}, \tag{25}$$

where $A_{\rm mag}$ is a constant. Nevertheless, for $\alpha \geqslant 1$ the series is nonstationary and the fluctuations at a given scale also depend on N. In Appendix A we show that the fluctuations in the sign series for $\alpha \geqslant 1$ can be written as

$$F_{\rm sign}(\ell) = B_{\rm sign}\frac{\ell^{\alpha_{\rm sign}}}{N^{\alpha_{\rm sign}-1}}, \tag{26}$$

where $B_{\rm sign}$ is a constant.

Clearly, the positive power of N ($\alpha_{\rm sign} - 1 > 0$) dividing in Eq. (26) makes $F_{\rm sign}(\ell) < F_{\rm mag}(\ell)$ at small scales while $F_{\rm sign}(\ell) > F_{\rm mag}(\ell)$ for large ones. This behavior also justifies the fact, commented on above, that at short scales the series scales with $\alpha_1 \simeq \alpha_{\rm sign}$ and $\alpha_2 \simeq \alpha_{\rm mag}$ for the larger ones.

Thus, the crossover will be located at the point $\ell_{\rm c}$ where the equality between (25) and (26) holds $F_{\rm mag}(\ell_{\rm c}) = F_{\rm sign}(\ell_{\rm c})$ and then

$$\ell_{\rm c} = \frac{A_{\rm mag}}{B_{\rm sign}}N^{\frac{\alpha_{\rm sign}-1}{\alpha_{\rm sign}-\alpha_{\rm mag}}} \propto N^{k}, \tag{27}$$

where

$$k = \frac{\alpha_{\rm sign}-1}{\alpha_{\rm sign}-\alpha_{\rm mag}}. \tag{28}$$

The analytical results obtained in Eqs. (27) and (28) are in good agreement with the simulations shown in Fig. 8. It is worth mentioning that $k < 1$, provided that $\alpha_{\rm mag} < 1$. This means that $\ell_{\rm c}$ grows slower than the size of the system, and thus the crossover will always be observable for long enough series.

C. Case $\alpha_{\rm sign} > 1, \alpha_{\rm mag} > 1$

In this case $F(\ell)$ might also present a crossover, although it will be difficult to observe in practice. To better understand the behavior of $F(\ell)$ in this regime we follow a procedure similar to that described in the previous section. As well as in the previous section, $\alpha_{\rm sign} > 1$, and we have for the fluctuations in the sign

$$F_{\rm sign}(\ell) = B_{\rm sign}\frac{\ell^{\alpha_{\rm sign}}}{N^{\alpha_{\rm sign}-1}}. \tag{29}$$

Now, in addition, the magnitude series is also nonstationary ($\alpha_{\rm mag} > 1$), and, from the definition of fractional Brownian motion, the variance of the series grows as $N^{2(\alpha_{\rm mag}-1)}$. This means that, in order to keep the series with unit standard deviation, the generation procedure (Sec. II C) carries out an

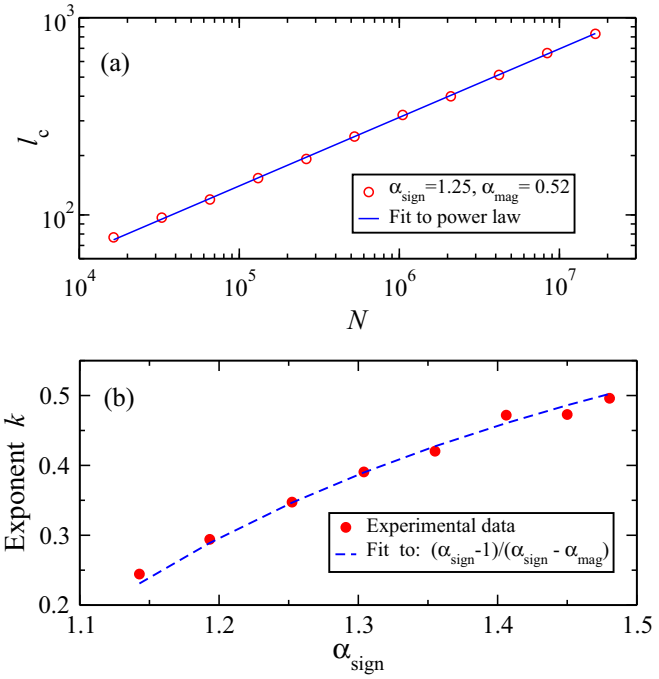

FIG. 8. Position of the crossover $\ell_{\rm c}$ as a function of the size of the series N. (a) To check that ℓ grows as a power law of the system size N (27), we generate series with $\alpha_{\rm sign} = 1.25$ and $\alpha_{\rm mag} = 0.52$ and sizes in the range $[2^{13},2^{24}]$. For each size we obtain $F(\ell)$, average over 1000 series, and determine the position of the crossover $\ell_{\rm c}$ by fitting $F(\ell)$ to the derivative of a sigmoid [31]. This procedure also gives α_1 and α_2. The fit of the curve $\ell_{\rm c}$ vs N (open red circles) to a power law (solid blue line) gives an exponent $k = 0.345$ close to the value 0.342 predicted by (28). (b) We repeat the experiment for different values of $\alpha_{\rm sign}$ in the range [1,1.5] and obtain k for each one. Finally, we fit the curve of k vs $\alpha_{\rm sign}$ (closed red circles) to (28) (dashed blue line). The value obtained for $\alpha_{\rm mag} = 0.52$ coincides with the actual value used for the simulations.

implicit division of the series by the factor $N^{\alpha_{\rm mag}-1}$ [32], and thus we will obtain for the fluctuations of the magnitude:

$$F_{\rm mag}(\ell) = B_{\rm mag}\frac{\ell^{\alpha_{\rm mag}}}{N^{\alpha_{\rm mag}-1}}. \tag{30}$$

Again, the position of the crossover will be given by the value $\ell_{\rm c}$ for which the fluctuations in the magnitude and sign reach the same value:

$$B_{\rm mag}\frac{\ell_{\rm c}^{\alpha_{\rm mag}}}{N^{\alpha_{\rm mag}-1}} = B_{\rm sign}\frac{\ell_{\rm c}^{\alpha_{\rm sign}}}{N^{\alpha_{\rm sign}-1}}, \tag{31}$$

$$\ell_{\rm c} = N\left(\frac{B_{\rm mag}}{B_{\rm sign}}\right)^{\frac{1}{\alpha_{\rm sign}-\alpha_{\rm mag}}} \propto N. \tag{32}$$

This means that the position of the crossover grows proportionally to the size of the series.

Here is important to point out that the normalization described above results in a reduction of the fluctuations at short scales [32]. This reduction becomes more evident as α increases, and thus, at short scales ($\ell \ll \ell_{\rm c}$), the fluctuations are governed by the smallest exponent $\alpha_1 = \min\{\alpha_{\rm mag},\alpha_{\rm sign}\}$, while at large scales ($\ell \gg \ell_{\rm c}$) the correlation exponent will be given by $\alpha_2 = \max\{\alpha_{\rm mag},\alpha_{\rm sign}\}$.

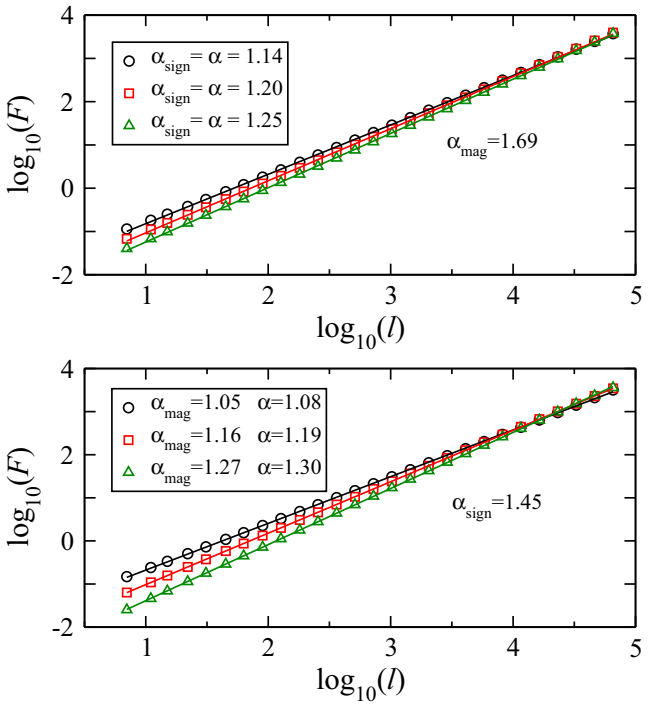

FIG. 9. Example of composed series generated by multiplying sign and magnitude from independent original series for $\alpha_{\text{mag}} > 1$ and $\alpha_{\text{sign}} > 1$. In this region we do not observe crossover (see text). (a) Example of series with $\alpha_{\text{sign}} < \alpha_{\text{mag}}$. The exponent of correlation of the composed series reaches the value α_{sign} ($\min\{\alpha_{\text{mag}},\alpha_{\text{sign}}\}$) for each series. (b) Example of series with $\alpha_{\text{sign}} > \alpha_{\text{mag}}$. The correlations in the composed series are mainly controlled by those in the magnitude, although the exponent of correlation is slightly higher. This effect becomes more noticeable as the difference between both magnitude and sign exponents of correlation decreases because in these cases, the crossover is less sharp, thus there is a small contribution of the regime after the transition.

In order to find out the values of ℓ_{c} we have systematically generated pairs of correlated series of signs and magnitudes with $\alpha_{\text{mag}} \in (1,2)$ and $\alpha_{\text{sign}} \in (1,1.5)$, and for each of them we obtain α_{mag},α_{sign}, B_{mag}, and B_{sign} and evaluate ℓ_{c} by using (32). We find two different regions (Fig. 9):

(i) $\alpha_{\text{mag}} \geqslant \alpha_{\text{sign}}$. In this case, in all experiments we obtain $\ell_{\text{c}} > N$, implying that the crossover is not reachable.

(ii) $\alpha_{\text{mag}} < \alpha_{\text{sign}}$. Here in a few situations we obtain $\ell_{\text{c}} \leqslant N$ although the values of $F_{\text{mag}}(\ell)$ and $F_{\text{sign}}(\ell)$ are too close to display a clear crossover. In addition, only values of $\ell_{\text{c}} \leqslant N/10$ can be observed in practice because DFA is computed, as usual, up to $N/10$ [17].

In conclusion, we barely observe crossovers within this region, and the composed series will show a single scaling in the whole range, the correlation exponent being $\alpha = \alpha_1 \simeq \min\{\alpha_{\text{mag}},\alpha_{\text{sign}}\}$.

Another conclusion we can extract from this case is that it is not possible to generate series with an exponent of correlation greater than $\alpha = 1.5$ when composing series by means of independent magnitudes and signs. We try to obtain the greatest possible exponent for composed series, by using $\alpha_{\text{in}} = 2$ for the magnitude ($\alpha_{\text{mag}} \simeq 1.9$) and $\alpha_{\text{in}} = 2$ for the sign ($\alpha_{\text{sign}} \simeq 1.5$). Then we compose each pair of magnitude and sign series, obtain α of the composed series, and represent the distribution. The results (Fig. 10) show a distribution with a sharp peak at $\alpha = 1.5$ ($\min\{\alpha_{\text{mag}},\alpha_{\text{sign}}\}$) in agreement with what we explained previously. By visual inspection, the few series we have observed with $\alpha > 1.5$ correspond to situations where the scaling of the composed series is not very good, together with those few situations where the crossover is observable. Last, Table I summarizes the results obtained in this section.

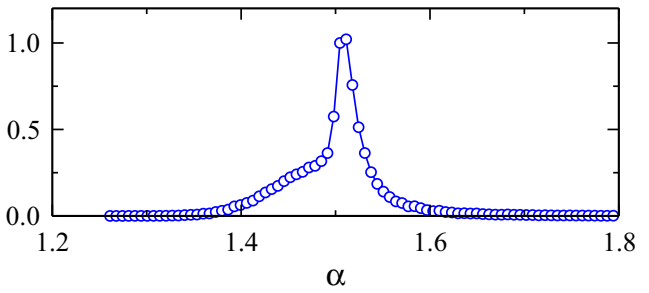

FIG. 10. Distribution of exponents of series obtained with $\alpha_{\text{mag}} \simeq 1.9$ and $\alpha_{\text{sign}} \simeq 1.5$. The size of the series is 2^{20}, and results are averaged over 10^5 series.

V. MULTIFRACTAL PROPERTIES OF COMPOSED SERIES

In the previous section we studied only linear correlations of the composed series. However, it has been reported [4,5] that series with correlated magnitude ($\alpha_{\text{mag}} > 0.5$) and uncorrelated sign ($\alpha_{\text{sign}} = 0.5$) also present nonlinear correlations (multifractal properties). Thus, in this section we analyze the multifractal properties of the composed series.

However, our results for composed series presented in Sec. IV indicate the existence of crossovers in the scaling at ℓ_c whenever $\alpha_{\text{sign}} > 1$. Such behavior could lead to the existence of two different multifractal spectra below and above ℓ_{c}. Furthermore, it is not even guaranteed that $\ell_c = \text{const}$ for the different moments of order q, thus precluding a straightforward calculation of both spectra.

For this reason, we restrict ourselves to the regime $\alpha_{\text{sign}} < 1$ where, first, the composed time series posses single scaling and, second, the linear correlations in the composed time series are directly controlled by the sign series ($\alpha = \alpha_{\text{sign}}$). In addition, we have observed that when $\alpha_{\text{mag}} > 1.2$, there are numerical instabilities when calculating the multifractal spectra of composed series. Then we study here the multifractal

TABLE I. Results obtained for composition of independent magnitudes and signs.

α_{sign}	α_{mag}	α	Crossover
<1	[0.5,2]	α_{sign}	No
>1	<1	$\ell < \ell_{\text{c}}$ $\alpha_1 = \alpha_{\text{mag}}$	$\ell_{\text{c}} \propto N^k$
		$\ell > \ell_{\text{c}}$ $\alpha_2 = \alpha_{\text{sign}}$	$k = \frac{\alpha_{\text{sign}}-1}{\alpha_{\text{sign}}-\alpha_{\text{mag}}}$
>1	>1	$\min\{\alpha_{\text{mag}},\alpha_{\text{sign}}\}$	Not observable

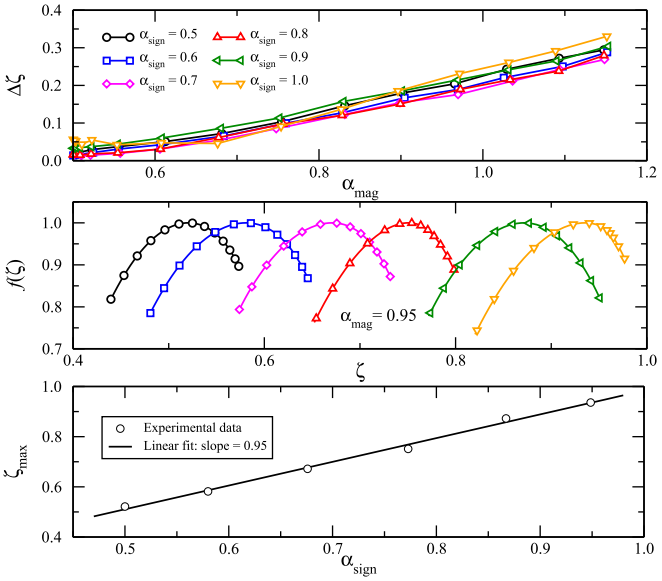

FIG. 11. (a) Relation between $\Delta\zeta$ and $\alpha_{\rm mag}$ of composed series by means of independent magnitudes and signs. $\Delta\zeta$ increases linearly with $\alpha_{\rm mag}$ when the magnitude series leave the uncorrelated regime ($\alpha_{\rm mag} > 0.5$), whereas $\alpha_{\rm sign}$ does not play an important role in the value of $\Delta\zeta$. Series are 2^{18} long, and results are averaged over an ensemble of 50 series. (b) Example of multifractal spectra of 2^{18} long series with $\alpha_{\rm mag} = 0.95$ and $\alpha_{\rm sign}$ in the interval $[0.5,1]$. To obtain the multifractral spectra, the MFDFA analysis (5) has been carried out for moments $q \in [-5,5]$. Despite varying $\alpha_{\rm sign}$, $\Delta\zeta$ is practically the same for all cases. Spectra are centered in $\zeta_{\rm max} \simeq \alpha_{\rm sign}$. (c) Relation between $\alpha_{\rm sign}$ and $\zeta_{\rm max}$ for the multifractal spectra obtained in (b). The data were linearly fitted with slope 0.95.

properties of composed time series with $\alpha_{\rm mag}$ and $\alpha_{\rm sign}$ in the intervals $[0.5,1.2]$ and $[0.5,1]$ respectively.

Specifically, we calculate the multifractal spectrum for each composed series using MFDFA (see Sec. II B) and study systematically two properties: the width of the multifractal spectrum, $\Delta\zeta$, and the location of its center, $\zeta_{\rm max}$.

Concerning the properties of the spectral width, we observe that $\Delta\zeta$ depends only on $\alpha_{\rm mag}$, and it is practically independent of the $\alpha_{\rm sign}$ value. Both properties are shown in Fig. 11(a), where we also notice that the dependence of $\Delta\zeta$ on $\alpha_{\rm mag}$ is essentially linear. This is an interesting property: given an input $\alpha_{\rm mag}$ value in the composition, we control directly the strength of the nonlinearities of the composed time, since such strength is quantified by $\Delta\zeta$.

We also study how the linear correlations present in the composed series, which are controlled by $\alpha_{\rm sign}$ ($\alpha = \alpha_{\rm sign}$), affect the location of the center of the multifractal spectrum, $\zeta_{\rm max}$. We observe that, for a fixed $\alpha_{\rm mag}$ value (and then for constant $\Delta\zeta$), the whole multifractal spectrum is displaced proportionally to the $\alpha_{\rm sign}$ value [see Fig. 11(b)]. Indeed, if we calculate numerically the location of the center of the spectrum, $\zeta_{\rm max}$, we obtain a very good linear dependence of $\zeta_{\rm max}$ on $\alpha_{\rm sign}$ [Fig. 11(c)], with slope $\simeq 1$.

In conclusion, the multifractal properties of composed time series obtained by multiplying independent magnitude and signs are completely controlled by only two parameters, the correlation exponents $\alpha_{\rm sign}$ and $\alpha_{\rm mag}$. While the first one controls the linear correlations of the composed series (α) and the location of the center of the multifractal spectrum ($\zeta_{\rm max}$), the second quantifies the width of the spectrum ($\Delta\zeta$) and then the strength of the nonlinearities in the composed series. Obviously this procedure can be used as an algorithm for the generation of complex artificial time series possessing not only prescribed linear long-range correlations (as FFM) but also controlled multifractal properties.

VI. CONCLUSIONS

We have presented a systematic study of the correlation properties of the decomposition of artificial long-range power-law linearly correlated time series into their magnitude and sign series as well as the correlation properties, including nonlinear ones, of the composed series obtained as products of independent magnitude and sign series.

Regarding the decomposition problem, we have studied the correlations of the magnitude and sign of a variety of fractional Gaussian noises and fractional Brownian motions generated by means of the Fourier Filtering Method, one of the most widely used to generate artificial linear correlated series. The results are summarized in Fig. 3. In addition, we have obtained analytical expressions for the correlation exponent of the sign series $\alpha_{\rm sign}$ [Eq. (16)]. In particular, we show that $\alpha_{\rm sign} \leqslant 3/2$ independently of the correlations of the original series. These results, together with those obtained here numerically for the magnitude shown in Fig. 3 (also in agreement with Kalisky *et al.* [5] for the square of the series), will be of great help in order to model surrogate time series. For example, the sign series obtained from the decomposition are often used to generate correlated binary series in the study of DNA sequences [13,25,30] or disordered binary solids [33] as well as to generate distributions of first-passage times of correlated series [6]. It is also worth mentioning that, following the results shown in Sec. III, it is clear that long-range anticorrelated binary sequences cannot be obtained using this method, a drawback shared with other methods [26–28].

Apart from the utility of the decomposition to generate surrogate series, the comparison of the results obtained here for artificial linear series with those obtained from real data would help to unveil the existence of coupling in the mechanisms responsible for the magnitude and sign of the increments or to discard it. This information is instrumental for the study of the underlying processes generating complex nonlinear time series such as those obtained from physiological systems.

By means of the composition, we studied the correlations in series obtained as the product of independent series of correlated magnitudes and signs.

First, we explore the linear correlations as measured by the DFA exponent and find that, only for those composed series with $\alpha_{\rm sign} < 1$, we obtain a scale-free behavior, i.e., a fit to a single power law of $F(\ell)$ in the whole range. In addition, the correlation exponent of the composition is given by $\alpha_{\rm sign}$ independently of $\alpha_{\rm mag}$. On the other hand, for $\alpha_{\rm sign} \geqslant 1$, we observe clear crossovers for $\alpha_{\rm mag} < 1$ whose position, ℓ_c, can be obtained analytically [Eq. (27)]. Here the composed signal scales with $\alpha_1 \simeq \alpha_{\rm mag}$ for $\ell < \ell_c$ whereas for $\ell > \ell_c$ it scales with $\alpha_2 \simeq \alpha_{\rm sign}$. For $\alpha_{\rm mag} \geqslant 1$ we show that the crossovers, although theoretically predicted, are difficult

to detect in practice and the composed signal approximately scales with a single exponent given by $\alpha_1 = \min\{\alpha_{\rm mag}, \alpha_{\rm sign}\}$. As a consequence of this and taking into account that $\alpha_{\rm sign} \leqslant 3/2$, the composition cannot produce signals with correlation exponents above $3/2$. Results are summarized in Table I.

Finally, we analyze the nonlinear properties of the composed signals by means of MFDFA in the region $\alpha_{\rm sign} < 1$. As a measure of the nonlinearity in the signal we use the width of the multifractal exponent ($\Delta\zeta$) and show that it grows almost linearly with $\alpha_{\rm mag}$, thus indicating that the nonlinear properties of the composed signals are controlled by the correlations in the magnitude. In addition, we also find that $\Delta\zeta$ is independent of $\alpha_{\rm sign}$. This last result is interesting because it means that we can generate surrogate signals for which we can fix both the linear correlations ($\alpha_{\rm sign}$) and the strength of the nonlinearity ($\Delta\zeta$).

ACKNOWLEDGMENTS

This work is partially supported by grants FQM-7964 from the Spanish Junta de Andalucía and FIS2012-36282 from the Spanish Government. We acknowledge support from the W. M. Keck Foundation, National Institutes of Health (NIH Grant No. 1R01- HL098437), Office of Naval Research (ONR Grant No. 000141010078), and US-Israel Binational Science Foundation (BSF Grant No. 2012219).

APPENDIX A: FLUCTUATIONS OF THE SIGN OF NONSTATIONARY SERIES ($\alpha \geqslant 1$)

Let us consider a long-range fractal correlated series with $\alpha \geqslant 1$ (fBM), if we denote as x the size of a segment without changes of sign inside it (i.e., segments of constant sign, or simply "segments"), it is known [6] that the distribution of x follows a power law with exponent $\alpha - 3$, which, once normalized, can be written as

$$p(x) = \frac{(2-\alpha)N^{2-\alpha}}{N^{2-\alpha}-1} x^{\alpha-3}. \tag{A1}$$

The mean value $\langle x \rangle$ of the constant-sign segments will be given by

$$\langle x \rangle = \int_1^N p(x)\,dx = \left(\frac{2-\alpha}{\alpha-1}\right)\frac{N-N^{2-\alpha}}{N^{2-\alpha}-1}, \tag{A2}$$

and the mean number of such segments inside a series of length N:

$$n = \frac{N}{\langle x \rangle} = \left(\frac{\alpha-1}{2-\alpha}\right)\frac{N^{2-\alpha}-1}{1-N^{1-\alpha}}. \tag{A3}$$

When evaluating the fluctuations at a given window size ℓ, only the portion of the signal covered by segments with $x < \ell$ will give a nonzero contribution: for the remainder of the signal the full window of size ℓ will be located inside a segment of constant sign, and then without internal fluctuation and its contribution to $F_{\rm sign}(\ell)$ will be zero [34].

In order to evaluate the portion of the signal covered by segments with $x < \ell$, first we evaluate the probability that a given segment is smaller than ℓ:

$$P(x<\ell) = \int_1^\ell p(x)\,dx = 1 - \frac{N^{2-\alpha}-\ell^{2-\alpha}}{\ell^{2-\alpha}[N^{2-\alpha}-1]}, \tag{A4}$$

the average size of those segments,

$$\langle x_{<\ell} \rangle = \frac{\int_1^\ell x\,p(x)\,dx}{P(x<\ell)} = \left(\frac{2-\alpha}{\alpha-1}\right)\frac{\ell^{\alpha-1}-1}{1-\ell^{\alpha-2}}, \tag{A5}$$

and the fraction of the series covered by segments with $x < \ell$:

$$f(x<\ell) = \frac{n\,P(x<\ell)\,\langle x_{<\ell}\rangle}{N} = \frac{\ell^{\alpha-1}-1}{N^{\alpha-1}-1} \simeq \frac{\ell^{\alpha-1}}{N^{\alpha-1}}. \tag{A6}$$

If we denote by i the number of 1's in a window of size ℓ it is straightforward to obtain that the variance of the window is given by

$$\mathrm{var}(i,\ell) = \frac{4i}{\ell} - \frac{4i^2}{\ell^2}. \tag{A7}$$

Taking into account that for N large enough we will find all possible values of $i \in \{1,2,\ldots,\ell-1\}$, we can assume that the averaged variance in windows of size ℓ located within segments with $x < \ell$ will be

$$\begin{aligned}\mathrm{var}(\ell) &= f(x<\ell)\langle \mathrm{var}(i,\ell)\rangle_i \\ &= \frac{\ell^{\alpha-1}}{N^{\alpha-1}}\frac{1}{\ell-1}\left(\frac{2}{3}\ell - \frac{2}{3\ell}\right) \propto \left(\frac{\ell}{N}\right)^{\alpha-1},\end{aligned} \tag{A8}$$

and the average standard deviation inside windows of size ℓ

$$\sigma(\ell) = \sqrt{\mathrm{var}(\ell)} \propto \left(\frac{\ell}{N}\right)^{\frac{\alpha-1}{2}}. \tag{A9}$$

$F_{\rm sign}(\ell)$ measures the rms fluctuations of the integrated signal with respect to ℓ and then

$$F_{\rm sign}(\ell) \propto \sigma(\ell)\,\ell \propto \frac{\ell^{\frac{1}{2}(\alpha+1)}}{N^{\frac{1}{2}(\alpha-1)}} = \frac{\ell^{\alpha_{\rm sign}}}{N^{\alpha_{\rm sign}-1}}, \tag{A10}$$

where $\alpha_{\rm sign} = \frac{1}{2}(\alpha+1)$ is the DFA exponent of the sign series for $1 \leqslant \alpha < 2$.

For higher values of α equations from (A1) to (A3) are no longer valid [6] and now the number of segments, n, is constant and independent of N. For a given window length ℓ, only n out of N/ℓ windows will contribute with nonvanishing variance, and thus we can write

$$\begin{aligned}\mathrm{var}(\ell) &= \frac{n\ell}{N}\langle \mathrm{var}(i,\ell)\rangle_i \\ &= \frac{n\ell}{N}\frac{1}{\ell-1}\left(\frac{2}{3}\ell - \frac{2}{3\ell}\right) \propto \frac{\ell}{N},\end{aligned} \tag{A11}$$

$$F_{\rm sign}(\ell) \propto \frac{\ell^{\frac{3}{2}}}{N^{\frac{1}{2}}} = \frac{\ell^{\alpha_{\rm sign}}}{N^{\alpha_{\rm sign}-1}}, \tag{A12}$$

where $\alpha_{\rm sign} = \frac{3}{2}$ is the DFA exponent of the sign series for $\alpha \geqslant 2$.

Note that both results [Eqs. (A10) and (A12)], agree with the fact that the fluctuations in a nonstationary series should depend on the size of the series, N.

APPENDIX B: AUTOCORRELATION FUNCTION OF A TIME SERIES WITH UNCOUPLED MAGNITUDE AND SIGN

The autocorrelation function of a time series $\{x_i\}$ at distance ℓ, normally distributed with zero mean and unit standard

deviation, is given by

$$C(\ell) = \frac{\langle x_i x_{i+\ell}\rangle - \langle x_i\rangle\langle x_{i+\ell}\rangle}{\sigma^2} = \langle x_i x_{i+\ell}\rangle, \tag{B1}$$

where $\langle\cdot\rangle$ denotes average over the series. Obviously we can write

$$C(\ell) = \langle \mathrm{sgn}(x_i)|x_i|\mathrm{sgn}(x_{i+\ell})|x_{i+\ell}|\rangle, \tag{B2}$$

$$C(\ell) = \langle \mathrm{sgn}(x_i)\mathrm{sgn}(x_{i+\ell})|x_i x_{i+\ell}|\rangle, \tag{B3}$$

where $\mathrm{sgn}(\cdot)$ denotes the sign function. If we consider that *magnitude and sign are not coupled* (i.e., they are independent random variables) we can assume that

$$C(\ell) = \langle \mathrm{sgn}(x_i)\mathrm{sgn}(x_{i+\ell})\rangle\langle|x_i x_{i+\ell}|\rangle, \tag{B4}$$

$$C(\ell) = C_{\mathrm{sign}}(\ell)\langle|x_i x_{i+\ell}|\rangle, \tag{B5}$$

where $C_{\mathrm{sign}}(\ell)$ is the autocorrelation function at distance ℓ of the sign time series. On the other hand, we can write for the autocorrelation function of the magnitude time series:

$$C_{\mathrm{mag}}(\ell) = \frac{\langle|x_i x_{i+\ell}|\rangle - \langle|x_i|\rangle\langle|x_{i+\ell}|\rangle}{\langle|x_i|^2\rangle - \langle|x_i|\rangle^2}, \tag{B6}$$

and, taking into account that $\{x_i\}$ are normally distributed with zero mean and unit variance, it follows that

$$\langle|x_i|\rangle = \sqrt{\frac{2}{\pi}} \quad \text{and} \quad \langle|x_i|^2\rangle = 1. \tag{B7}$$

Replacing in Eq. (B6) we get

$$\langle|x_i x_{i+\ell}|\rangle = \frac{(\pi-2)C_{\mathrm{mag}}(\ell)+2}{\pi}, \tag{B8}$$

and finally replacing $\langle|x_i x_{i+\ell}|\rangle$ in Eq. (B4):

$$C(\ell) = C_{\mathrm{sign}}(\ell)\frac{(\pi-2)C_{\mathrm{mag}}(\ell)+2}{\pi}. \tag{B9}$$

[1] P. Ch. Ivanov *et al.*, Multifractality in human heartbeat dynamics, Nature (London) **399**, 461 (1999).

[2] P. C. Ivanov *et al.*, Sleep-wake differences in scaling behavior of the human heartbeat: Analysis of terrestrial and long-term spacial flight data, Europhys. Lett. **48**, 594 (1999).

[3] Y. Ashkenazy, P. C. Ivanov, S. Havlin, C.-K. Peng, A. L. Goldberger, and H. E. Stanley, Magnitude and Sign Correlations in Heartbeat Fluctuations, Phys. Rev. Lett. **86**, 1900 (2001).

[4] Y. Ashkenazy *et al.*, Magnitude and sign scaling in power-law correlated time series, Physica A **323**, 19 (2003).

[5] T. Kalisky, Y. Ashkenazy, and S. Havlin, Volatility of linear and nonlinear time series, Phys. Rev. E **72**, 011913 (2005).

[6] C. Carretero-Campos, P. Bernaola-Galván, P. Ch. Ivanov, and P. Carpena, Phase transitions in the first-passage time of scale-invariant correlated processes, Phys. Rev. E **85**, 011139 (2012).

[7] L. Zhu *et al.*, Magnitude and sign correlations in conductance fluctuations of horizontal oil water two-phase flow, J. Phys. Conf. Ser. **364**, 012067 (2012).

[8] H. A. Makse, G. W. Davies, S. Havlin, P. Ch. Ivanov, P. R. King, and H. E. Stanley, Long-range correlations in permeability fluctuations in porous rock, Phys. Rev. E **54**, 3129 (1996).

[9] H. A. Makse, S. Havlin, P. Ch. Ivanov, P. R. King, S. Prakash, and H. E. Stanley, Pattern formation in sedimentary rocks: Connectivity, permeability, and spatial correlations, Physica A **233**, 587 (1996).

[10] I. Bartos and I. M. Jánosi, Nonlinear correlations of daily temperature records over land, Nonlin. Processes Geophys. **13**, 571 (2006).

[11] Q. Li, Z. Fu, N. Yuan, and F. Xie, Effects of non-stationarity on the magnitude and sign scaling in the multi-scale vertical velocity increment, Physica A **410**, 9 (2014).

[12] Y. Liu, P. Gopikrishnan, P. Cizeau, M. Meyer, C. K. Peng, and H. E. Stanley, Statistical properties of the volatility of price fluctuations, Phys. Rev. E **60**, 1390 (1999).

[13] C.-K. Peng, S. V. Buldyrev, S. Havlin, M. Simons, H. E. Stanley, and A. L. Goldberger, Mosaic organization of DNA nucleotides, Phys. Rev. E **49**, 1685 (1994).

[14] P. Allegrini, M. Barbi, P. Grigolini, and B. J. West, Dynamical model for DNA sequences, Phys. Rev. E **52**, 5281 (1995).

[15] G. M. Molchan, Maximum of fractional Brownian motion: Probabilities of small values, Comm. Math. Phys. **205**, 97 (1999).

[16] G. Rangarajan and M. Z. Ding, Integrated approach to the assessment of long range correlation in time series data, Phys. Rev. E **61**, 4991 (2000).

[17] K. Hu, P. C. Ivanov, Z. Chen, P. Carpena, and H. E. Stanley, Effect of trends on detrended fluctuation analysis, Phys. Rev. E **64**, 011114 (2001).

[18] L. Xu, P. C. Ivanov, K. Hu, Z. Chen, A. Carbone, and H. E. Stanley, Quantifying signals with power-law correlations: A comparative study of detrended fluctuation analysis and detrended moving average techniques, Phys. Rev. E **71**, 051101 (2005).

[19] Q. D. Y. Ma, R. P. Bartsch, P. Bernaola-Galván, M. Yoneyama, and P. C. Ivanov, Effects of extreme data loss on detrended fluctuation analysis, Phys. Rev. E **81**, 031101 (2010).

[20] Z. Chen, P. C. Ivanov, K. Hu, and H. E. Stanley, Effect of nonstationarities on detrended fluctuation analysis, Phys. Rev. E **65**, 041107 (2002).

[21] Z. Chen, K. Hu, P. Carpena, P. Bernaola-Galvan, H. E. Stanley, and P. C. Ivanov, Effect of nonlinear filters on detrended fluctuation analysis, Phys. Rev. E **71**, 011104 (2005).

[22] Y. Xu *et al.*, Effects of coarse-graining on the scaling behavior of long-range correlated and anti-correlated signals, Physica A **390**, 4057 (2010).

[23] J. W. Kantelhardt *et al.*, Multifractal detrended fluctuation analysis of nonstationary time series, Physica A **316**, 87 (2002).

[24] H. A. Makse, S. Havlin, M. Schwartz, and H. E. Stanley, Method for generating long-range correlations for large systems, Phys. Rev. E **53**, 5445 (1996)

[25] P. Bernaola-Galván, J. L. Oliver, M. Hackenberg, A. V. Coronado, P. Ch. Ivanov, and P. Carpena, Segmentation of time series with long-range fractal correlations, Eur. Phys. J. B **85**, 211 (2012).

[26] F. M. Izrailev, A. A. Krokhin, N. M. Makarov, and O. V. Usatenko, Generation of correlated binary sequences from white noise, Phys. Rev. E **76**, 027701 (2007).

[27] O. V. Usatenko, S. S. Melnik, S. S. Apostolov, N. M. Makarov, and A. A. Krokhin, Iterative method for generating correlated binary sequences, Phys. Rev. E **90**, 053305 (2014).

[28] S. Hod and U. Keshet, Phase transition in random walks with long-range correlations, Phys. Rev. E **70**, 015104(R) (2004).

[29] S. S. Apostolov, F. M. Izrailev, N. M. Makarov, Z. A. Mayzelis, S. S. Melnyk, and O. V. Usatenko, The Signum function method for the generation of correlated dichotomic chains, J. Phys. A: Math. Theor. **41**, 175101 (2008).

[30] P. Bernaola-Galván, P. Carpena, R. Roman-Roldán, and J. L. Oliver, Study of statistical correlations in DNA sequences, Gene **300**, 105 (2002).

[31] P. Carpena, J. Aguiar, P. Bernaola-Galván, and C. Carnero-Ruiz, Problems Associated with the treatment of conductivity-concentration data in surfactant solutions: Simulations and experiments, Langmuir **18**, 6054 (2002).

[32] J. W. Kantelhardt, S. Russ, A. Bunde, S. Havlin, and I. Webman, Comment on "Delocalization in the 1D Anderson model with long-range correlated disorder," Phys. Rev. Lett. **84**, 198 (2000).

[33] P. Carpena, P. Bernaola-Galván, P. Ch. Ivanov, and H. E. Stanley, Metal-insulator transition in chains with correlated disorder, Nature (London) **418**, 955 (2002).

[34] To be precise, for each segment of constant sign with $x > \ell$ we will have at most two windows that partially belong to the segment, but, especially for $\alpha > 1$, this effect will be negligible.